

11-1-1994

# DESIGN AND ANALYSIS OF TRANSMITTER DIVERSITY USING INTENTIONAL FREQUENCY OFFSET FOR WIRELESS COMMUNICATIONS

Wen-yi Kuo

*Purdue University School of Electrical Engineering*

Michael P. Fitz

*Purdue University School of Electrical Engineering*

Follow this and additional works at: <http://docs.lib.purdue.edu/ecetr>

---

Kuo, Wen-yi and Fitz, Michael P, "DESIGN AND ANALYSIS OF TRANSMITTER DIVERSITY USING INTENTIONAL FREQUENCY OFFSET FOR WIRELESS COMMUNICATIONS" (1994). *ECE Technical Reports*. Paper 204.

<http://docs.lib.purdue.edu/ecetr/204>

This document has been made available through Purdue e-Pubs, a service of the Purdue University Libraries. Please contact [epubs@purdue.edu](mailto:epubs@purdue.edu) for additional information.

DESIGN AND ANALYSIS OF  
TRANSMITTER DIVERSITY USING  
INTENTIONAL FREQUENCY OFFSET  
FOR WIRELESS COMMUNICATIONS

WEN-YI KUO  
MICHAEL P. FITZ

TR-EE 94-35  
NOVEMBER 1994



SCHOOL OF ELECTRICAL ENGINEERING  
PURDUE UNIVERSITY  
WEST LAFAYETTE, INDIANA 47907-1285

**DESIGN AND ANALYSIS OF TRANSMITTER  
DIVERSITY USING INTENTIONAL FREQUENCY  
OFFSET FOR WIRELESS COMMUNICATIONS \***

*Wen-yi Kuo and Michael P. Fitz*

School of Electrical Engineering  
Purdue University  
West Lafayette, IN 47907-1285

email: [wenyi@ecn.purdue.edu](mailto:wenyi@ecn.purdue.edu), [mpfitz@ecn.purdue.edu](mailto:mpfitz@ecn.purdue.edu)

*FAX: (317)-494-6440*

---

\*

This work supported by NSF under Grant NCR 9115820.

## TABLE OF CONTENTS

	Page
LIST OF FIGURES .....	iii
ABSTRACT.....	iv
I. INTRODUCTION .....	1
II. ANALYTICAL MODELS.....	4
A. Signals Models.....	4
B. Transmitter Diversity with Intentional Frequency Offset .....	6
C. Models for L-Diversity with Intentional Frequency Offset .....	7
III. PERFORMANCE ANALYSIS OF CODED MODULATION WITH PSAM .....	10
A. Optimal Decoding / Demodulation.....	10
B. Traditional Union Bound.....	11
C. Progressive Union Bound.....	13
IV. PERFORMANCE OF TRANSMITTER DIVERSITY .....	18
A. Achieving Ideal Interleaving.....	18
A-1 Comparison between BCM and TCM for ideal interleaving .....	20
B. Non-ideal Interleaving Performance.....	20
B-1. Example of BCM1.....	21
B2 . Example of TCM1.....	22
B-3 Degradation caused by Ideal Interleaving Assumption.....	22
V. CONCLUSION .....	28
LIST OF REFERENCES.....	29

## LIST OF FIGURES

Figure	Page
1. The block diagram of the system with transmitter diversity and PSAM.....	9
2. Bounding errors in various fading rates.....	16
3. Bounding errors in stationary fading ( $f_D=0$ ) .....	17
4. Autocorrelation of the MD process in stationary fading.....	24
5. The effect of frequency offset and interleaving depth in stationary fading.....	24
6. Performance gain of transmitter diversity for BCM1 in stationary fading .....	25
7. The effect of frequency offset and interleaving depth in stationary fading for TCMI .....	25
8. Performance gain of using transmitter diversity for the TCMI in stationary fading .....	26
9. Performance degradation caused by the assumption of ideal interleaving for BCM1 .....	26
10. Performance degradation caused by the assumption of ideal interleaving for the TCMI .....	27

## ABSTRACT

Coded modulation (usually with interleaving) is used in fading channel **communications** to achieve good error performance. The major benefit from using coded modulation in fading channels is achieved if each code symbol of a **codeword** (or coded sequence) suffers statistically different fading (preferably independent fading). However, in many applications of mobile communications (e.g. in a metropolitan environment), a low vehicle speed (and hence a small Doppler spread) is very common. With a small Doppler spread, ideal or close-to-ideal interleaving is no longer feasible and all **code** symbols of a **codeword** would suffer highly correlated fading especially in stationary fading (Doppler spread=0). Coded modulations will thus suffer seriously degraded **performance**. The transmitter diversity using intentional frequency offset between antennas can generate the necessary time-varying fading and maintain the effectiveness of the **coded** signaling scheme. This work found that proper selections of the intentional frequency offset and interleaving depth can achieve less correlated fading or even independent fading (if enough antennas are used). Previous performance analysis based on ideal interleaving is not sufficient for slow fading cases and this work establishes the performance analysis of coded **modulation** in fading channels for a more general case which **permits** correlated fading **and** pilot symbol assisted modulation. Also the prevalent union **bound** is found of large bounding errors in slow fading environments and an improved union bound is **presented** to assess the close-to-actual error performance.

## I. Introduction

Coded modulation is often used in the fading channel communications to achieve robust performance and good power and bandwidth efficiency. The use of trellis coded modulation (TCM) in fading channels has been proposed by many authors (e.g., [1]) and performance analyses with various assumptions on the demodulator structure are presented in [2-4]. Block coded modulation (BCM) has similarly been proposed for fading channel communications (e.g., [5-7]). In fading channels, the Hamming distance of a code is more significant than its minimum Euclidean distance [3] if ideal interleaving is achieved. Hence if a BCM code can provide the same Hamming distance and throughput rate as a TCM code, they should achieve nearly equivalent performance in fading channels. The major benefit of using coded modulation (usually combined with interleaving) in fading channels is that time diversity can be achieved so that each code symbol of a codeword suffers a statistically different fading distortion (preferably independent fading). Burst errors (typically caused by a deep fade) are thus spread over many different codewords and the error correcting function of a code can then be fully utilized.

Most work in this area assumes that the fading rate of the channel is fast enough to make the ideal or quasi-ideal interleaving possible. For example, the analysis in [2] assumes ideal interleaving and the analysis in [4] assumes the fading is fast enough to make the saddle point approximation valid. Often in practice the fading is very slow and a practical interleaving depth cannot provide independent fading. This is especially true for pedestrian (e.g., pagers, cellular phones, etc.) or slow moving vehicle communication applications where a very small fading rate (Doppler spread) is usually encountered. In

these situations, ideal interleaving (and thus independent fading for each code symbol) is usually not an appropriate assumption and a more detailed treatment **accounting** for finite interleaving and correlated fading is needed. Also the prevalent union bound of bit error probability (BEP) for coded modulations is found only to provide a loose **bound** in a slow fading situation. An improved union bound will be presented to reduce the bounding **errors**.

Spatial diversity is a well known technique to improve the error performance for **communications** over fading channels. While techniques of receiver spatial diversity are well **developed**, techniques of transmitter spatial diversity have not received equivalent attention. For portable communications, applications of receiver diversity are very limited or even not feasible due to the physical constraint on the portable receivers. In these cases, improving performance by using transmitter spatial diversity is a more **appropriate** approach. Recent research [8-10] showed that properly designed transmitter diversity techniques can achieve significant performance improvement. Furthermore, using **transmitter** diversity techniques in combination with receiver diversity techniques can **attain** the best **tradeoff** between amount of diversity and complexity. This work investigates the transmitter diversity using intentional frequency offset between transmitters to produce time-varying fading even on a channel with no Doppler spread. This technique can achieve near ideal interleaving (*i.e.*, each code symbol suffers less dependent fading) previously not feasible for slow fading **applications** by proper selections of the intentional frequency offset and interleaving depth.

**This** paper addresses two principle issues of importance for digital commnucations in a wireless mobile environment. First, the performance of coded **modulation** with pilot symbol assisted modulation (PSAM) is examined. The novelty of this **work** is that it **accounts** for the finite interleaving and the correlated fading inside a codeword. Improved union bounds on the BEP needed for analysis in slow fading are also presented. Second, the transmitter spatial diversity technique using intentional frequency offset to

produce enforced time-varying fading is fully investigated. Design criteria to achieve ideal **interleaving** and improve error performance in slow fading are introduced.

This paper begins with Section **II** introducing the signal models. Section **III** develops the BEP performance analysis tools. In Section **IV**, the effect of **using** intentional frequency offset in transmitter diversity with coded modulation is investigated. Section **V** concludes.

## II. Analytical Models

### A. Signals Models

Fig. 1 is a block diagram of our analytical system model. The coded modulator transforms the input binary random data into a sequence of M-QAM or M-PSK symbols denoted as  $d_k$ . The sequence of modulation symbols is then interleaved before being linearly modulated on the carrier and transmitted.

In this paper, to demonstrate the characteristics of transmitter diversity with intentional frequency offset, we consider a simple BCM and a simple TCM. The BCM considered (denoted BCM1) is a simple repetition code which has codewords of the form

$$\begin{aligned} \mathbf{d}_l &= [d_{l1}, d_{l2}, d_{l3}] \\ &= \sqrt{\frac{2}{5}} \left[ \left( (2I_l^{(1)} + I_l^{(2)}) + j(2I_l^{(3)} + I_l^{(4)}) \right), \left( (2I_l^{(4)} + I_l^{(3)}) + j(2I_l^{(2)} + I_l^{(1)}) \right), \left( (2I_l^{(3)} + I_l^{(2)}) + j(2I_l^{(4)} + I_l^{(1)}) \right) \right] \end{aligned} \quad (1)$$

where  $I_l^{(i)}$  is the  $i$ th input information bit to the encoder at time  $l$  (the  $l$ th block) and  $I_l^{(i)}$  takes the value of  $\pm 1$ . BCM1 takes 4 input binary bits as an input block and outputs 3 16-QAM symbols (rate=1/3). The Hamming distance of this code is equal to 3 since any pair among the 16 codewords of this code always have 3 different output symbols. This code provides more equal error protection than a simple repetition code since the information bits are scrambled into the in-phase and quadrature phase parts and are also distributed in the most significant bit (MSB) and the least significant bit (LSB) of the output symbols. The TCM considered in this paper is the simple code for 16-QAM presented in [11] (denoted TCM1) which provides a minimum Hamming distance of 3.

This paper considers *narrowband* digital communications on land mobile channels and such channels are accurately modeled as imposing a time-varying multiplicative distortion (MD) process upon the transmitted signal. One significant problem in this

channel demodulation is to produce an estimate of the time-varying **MD** for demodulation. Common techniques for estimating the **MD** process are transmitted reference schemes such as **PSAM** [12-14] and tone calibration techniques [15-17]. These transmitted reference techniques provide better performance than differential detection [18, 19] in a fairly simple structure. This paper considers **PSAM** because of the simplicity and high performance. However, the revision to other types of transmitted reference synchronization is straightforward. The baseband equivalent of the transmitted signal has the form

$$s(t) = \sum_k \tilde{d}_k u(t - kT) \quad (2)$$

where  $u(t)$  represents a square root unit energy Nyquist pulse shape<sup>1</sup>,  $T$  is the symbol duration and  $\tilde{d}_k$  represents the modulation symbol which can either be a pilot modulation or a symbol from an interleaved codeword. The  $\tilde{d}_i$ 's are normalized such that  $E\{|\tilde{d}_i|^2\} = \log_2 M$ . The known pilot symbols of **PSAM** are inserted (one every  $P_{ins}$  symbols) in the transmitted symbols to help the demodulator derive a channel state estimate. For spectral shaping and interference suppression purposes, the values of the known pilot symbols are typically randomized [14] but for the analysis in this paper we will assume all pilot symbols have  $E\{|\tilde{d}_i|^2\} = \log_2 M$ .

The channel model for this paper is the frequency non-selective, time-varying, isotropic scattering, Rayleigh fading channel. With this channel, the input to the receiver is given by

$$z(t) = c(t)s(t) + n(t) \quad (3)$$

where  $c(t)$  is a zero mean complex Gaussian multiplicative distortion (**MD**) and  $n(t)$  is a zero mean complex AWGN process with one-sided spectral density  $N_0$ . The processes

---

<sup>1</sup>  $R_u(nT) = \int_{-\infty}^{\infty} u(t)u^*(t - nT)dt = \delta_n$

$n(t)$  and  $c(t)$  are independent of each other. The isotropic Rayleigh scattering assumption implies that  $c(t)$  is characterized by [20]

$$R_c(\tau) = E\{c(t)c^*(t-\tau)\} = E_b J_0(2\pi f_D \tau) \quad (4)$$

where  $f_D$  represents the Doppler spread,  $E_b$  is the average received energy per bit,  $J_0()$  is the Bessel function of the zeroth order, and the asterisk (\*) denotes the complex conjugate operation. In the simulations presented later in the paper, isotropic scattering (i.e., (4)) is generated by Jakes model [20]. Also note that in the remainder of this paper, the signal to noise ratio per information bit (SNR/bit) is defined as

$$\gamma_b = \frac{E_b}{N_0} \frac{P_{ins}}{P_{ins} - 1} \quad (5)$$

The first step in the demodulation process is to pass the received signal (2) through a filter matched to the pulse shape  $u(t)$ . This paper assumes perfect symbol timing recovery and a first-order approximation that the pulse shape is narrow compared to  $1/f_D$  so that the MD is approximately constant for a pulse duration and the ISI produced by the MD is negligible (see [21] for the situations when this is valid). The output of the de-interleaver (after the matched filter) is then

$$\begin{aligned} x_k &= De-interleave[\tilde{x}_k] = De-interleave\left[\int_{-\infty}^{\infty} z(t)u^*(t-kT)dt\right] \\ &= De-interleave[\tilde{d}_k \tilde{c}_k + \tilde{n}_k] = d_k c_k + n_k \end{aligned} \quad (6)$$

where  $c_k$  is a discrete time Gaussian process with  $E[c_k c_{k-m}^*] = R_c(mD_{iv}T)$ ,  $D_{iv}$  is the interleaving depth, and  $n_k$  is a complex white Gaussian noise sequence with variance  $N_0$ .

## B. Transmitter Diversity with Intentional Frequency Offset

In [2], it is assumed that the interleaving depth is large enough so that each code symbol of a codeword (or coded sequence) suffers independent multiplicative distortion. However, for cases that have a very small Doppler spread, the assumption of independent fading on each code symbol is no longer valid unless a very large size buffer is used.

This means all code symbols of a codeword would suffer highly correlated fading and a deep fade will seriously degrade the performance especially in a stationary fading ( $f_D \approx 0$ ) environment.

One possible solution to provide diversity against fading without increasing the receiver complexity is to employ transmitter diversity techniques. Research has found using intentional time offset [8] or frequency offset [10] in transmitting antennas can produce time-varying fading even on channels with no Doppler spread. However, using time offset in transmitting antennas requires an equalizer in the receiver and could significantly inflate the cost and complexity. For narrowband transmission where equalization is unnecessary, using intentional frequency offset in transmitting antennas is a better approach. Techniques of transmitter diversity using frequency offset dates back to [22, 23]. These early techniques require a bandwidth expansion of nearly  $1/T$ . Recent research by Hiroike [10] has proposed to use a phase sweeping technique which only requires a small bandwidth expansion. However, [10] only presented the idea assuming ideal demodulation and lacked a detailed analysis. This paper takes the transmitter diversity idea in [10] and provides the detailed performance analysis for coded modulation and PSAM.

### **C. Models for L-Diversity with Intentional Frequency Offset**

This section will establish the signal model for the performance analysis of transmitter diversity. Assume  $L$  spatially separated antennas are used to transmit the same signal with intentional different frequency offset in the carrier frequency of each transmitting antenna. The spatial separation between the transmitting antennas is assumed to be large enough to produce independent fading for each transmitting path and is also assumed to be small enough to make the assumption valid that all transmitting paths suffer the same delay. This assumption on the spatial separation of antennas is easily achieved for systems with high carrier frequencies (0.2-2GHz) which are typically

prevalent in mobile wireless communications.

The resulted baseband equivalent MD process in the receiver is then

$$c(t) = \frac{e^{-j2\pi f_o t}}{\sqrt{L}} \sum_{i=0}^{L-1} c_i(t) \exp\left[j \frac{4\pi f_o i t}{L-1}\right] \quad (7)$$

$c_i(t)$  represents the independent Rayleigh fading process for the propagation between the  $i$ th antenna and the receiver, and  $2f_o$  is the bandwidth expansion of the transmitter diversity system. Again we assume that each transmitting path is accurately modeled by independent isotropic scattering (achieving independence will depend on the link geometry). For cases of particular interest, the autocorrelation of the MD process  $c(t)$  is then

$$R_c(\tau) = E[c(t)c^*(t-\tau)] = E_b J_0(2\pi f_D \tau) \cos(2\pi f_o \tau), \text{ if } L=2 \quad (8)$$

$$R_c(\tau) = \frac{1}{3} E_b J_0(2\pi f_D \tau) [1 + 2 \cos(2\pi f_o \tau)], \text{ if } L=3 \quad (9)$$

and

$$R_c(\tau) = \frac{1}{4} E_b J_0(2\pi f_D \tau) \left[ 2 \cos(2\pi f_o \tau) + 2 \cos\left(\frac{2\pi f_o \tau}{3}\right) \right], \text{ if } L=4. \quad (10)$$

Notice that the difference in the autocorrelation of MD process for systems using transmitter diversity (7) or not is the terms  $\cos(2\pi f_o \tau)$  and  $\cos(2\pi f_o \tau/3)$  which provide the enforced time-varying fading effect. Also note if the intentional frequency offset is not used ( $f_o=0$ ), then the autocorrelation of MD reduces to (4) and this means no diversity gain is obtained.

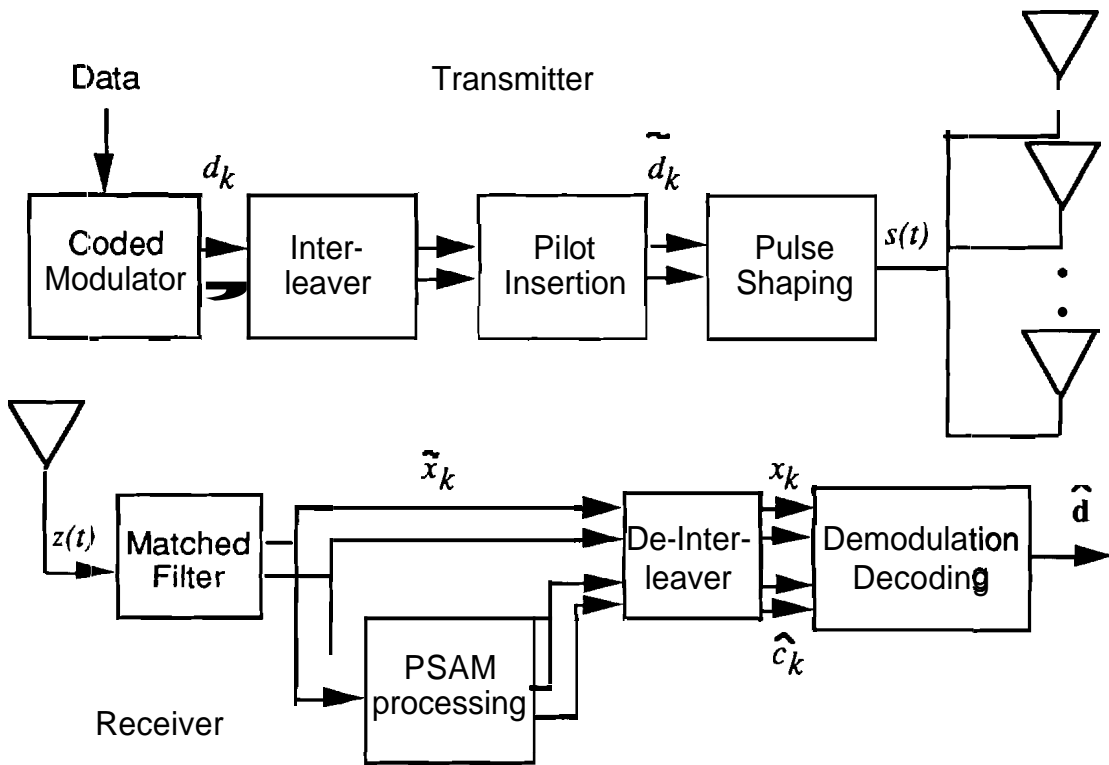


Fig. 1. The block diagram of the system with transmitter diversity and PSAM.

### III. Performance Analysis of Coded Modulation with PSAM

In this section, we derive the error performance of coded PSAM with transmitter diversity using intentional frequency offset.

#### A. Optimal Decoding I Demodulation

The major tasks of a fading channel receiver are first, to produce a channel state estimate  $\hat{c}_k$  and second, to demodulate/decode the transmitted message. In a PSAM demodulator, the  $2N$  matched filter output samples corresponding to pilot symbols which are nearest in time (before de-interleaving) to  $c_k$  are used to estimate  $c_k$ . These pilot samples are defined as

$$\tilde{\mathbf{x}}_p(k) = [\tilde{x}_{p1}, \tilde{x}_{p2}, \dots, \tilde{x}_{p2N}]^T = \mathbf{\Lambda}_p(k)\tilde{\mathbf{c}}_p(k) + \tilde{\mathbf{n}}_p(k) \quad (11)$$

where  $\mathbf{\Lambda}_p(k) = \text{diag}(\tilde{d}_{p1}, \tilde{d}_{p2}, \dots, \tilde{d}_{p2N})$ , and  $\tilde{\mathbf{c}}_p(k)$  is the associated MD vector of  $\tilde{\mathbf{x}}_p(k)$ .

The optimum (Wiener) filter for estimating the MD [13] is given as

$$\hat{c}_k = \mathbf{r}(k)\mathbf{R}_p^{-1}(k)\tilde{\mathbf{x}}_p(k) \quad (12)$$

where

$$\mathbf{r}(k) = E[\tilde{c}_k \tilde{\mathbf{x}}_p^H(k)] = E[\tilde{c}_k \tilde{\mathbf{c}}_p^H(k)]\mathbf{\Lambda}_p^*(k) \quad (13)$$

$$\mathbf{R}_p(k) = E[\tilde{\mathbf{x}}_p(k)\tilde{\mathbf{x}}_p^H(k)] = \mathbf{\Lambda}_p(k)E[\tilde{\mathbf{c}}_p(k)\tilde{\mathbf{c}}_p^H(k)]\mathbf{\Lambda}_p^*(k) + N_0\mathbf{I}_N$$

$E[\tilde{c}_l \tilde{c}_{l-m}^*] = R_c(mT)$  and  $c_k = \tilde{c}_{k'}$  ( $k'$  is the time index of  $k$  before de-interleaving).

Defining  $\mathbf{x}$  and  $\hat{\mathbf{c}}$  to be the deinterleaved matched filter output codeword or coded sequence and the associated deinterleaved MD estimate sequence respectively, the

optimal sequence (maximum likelihood) decoding rule takes the form<sup>2</sup>

$$\hat{\mathbf{d}} = \arg \max_{\mathbf{d}_i \in \Xi_d} \{p(\mathbf{d}_i|\hat{\mathbf{c}}, \mathbf{x})\} = \arg \max_{\mathbf{d}_i \in \Xi_d} \{f(\mathbf{x}|\hat{\mathbf{c}}, \mathbf{d}_i)\}. \quad (14)$$

where  $\mathbf{d}_i$  is a codeword or a coded sequence and  $\Xi_d$  is the space of all possible codewords (or coded sequences). From (6), the vector  $\mathbf{x}$  can be represented in the form

$$\mathbf{x} = \mathbf{\Lambda}_d \mathbf{c} + \mathbf{n} \quad (15)$$

where  $\mathbf{c}$  and  $\mathbf{n}$  are the MD sample vector and the noise sample vector respectively, and  $\mathbf{\Lambda}_d$  is the diagonal matrix whose diagonal elements contain the transmitted code symbols. For BCM, the length of the vectors in (15) are equal to the block length, while in TCM the vectors in (15) include the entire transmitted sequence. Since  $\mathbf{c}$  and  $\mathbf{n}$  are complex Gaussian, we can have the conditional moments of  $\mathbf{x}$  as

$$E[\mathbf{x}|\hat{\mathbf{c}}, \mathbf{d}_i] = E[\mathbf{\Lambda}_{d_i} \mathbf{c} + \mathbf{n}|\hat{\mathbf{c}}, \mathbf{d}_i] = \mathbf{\Lambda}_{d_i} E[\mathbf{c}|\hat{\mathbf{c}}] = \mathbf{\Lambda}_{d_i} \hat{\mathbf{c}} \quad (16)$$

$$\mathbf{C}_i = E\left[\left(\mathbf{x} - \mathbf{\Lambda}_{d_i} \hat{\mathbf{c}}\right)\left(\mathbf{x} - \mathbf{\Lambda}_{d_i} \hat{\mathbf{c}}\right)^H \middle| \hat{\mathbf{c}}, \mathbf{d}_i\right] = \mathbf{\Lambda}_{d_i} \mathbf{C}_c \mathbf{\Lambda}_{d_i}^H + N_0 \mathbf{I}_M \quad (17)$$

where

$$\mathbf{C}_c = E\left[(\mathbf{c} - \hat{\mathbf{c}})(\mathbf{c} - \hat{\mathbf{c}})^H\right] \quad (18)$$

denotes the covariance matrix of the estimate of the MD's. Thus the probability density function of  $\mathbf{x}$  is given as

$$f(\mathbf{x}|\hat{\mathbf{c}}, \mathbf{d}_i) = \left(\pi^{M_x} \det \mathbf{C}_i\right)^{-1} \exp\left[-\left(\mathbf{x} - \mathbf{\Lambda}_{d_i} \hat{\mathbf{c}}\right)^H \mathbf{C}_i^{-1} \left(\mathbf{x} - \mathbf{\Lambda}_{d_i} \hat{\mathbf{c}}\right)\right] \quad (19)$$

where  $M_x$  is the length of the sequence  $\mathbf{x}$ .

## B. Traditional Union Bound

Define the pairwise error event  $\{\mathbf{d}_i \rightarrow \mathbf{d}_j\}$  to be the event that the receiver makes the

---

<sup>2</sup>  $p(\bullet)$  and  $f(\bullet)$  indicate probability mass functions (pmf) and probability density functions (pdf) respectively.

decision that codeword  $\mathbf{d}_j$  is transmitted given the fact that codeword  $\mathbf{d}_i$  is actually transmitted. Then the bit error probability of a coded modulation can be obtained as

$$BEP = \sum_{\mathbf{d}_j \in \Xi_d} P\{\mathbf{d}_i \rightarrow \mathbf{d}_j\} \left( \frac{\text{number of error bits in event } \mathbf{d}_i \rightarrow \mathbf{d}_j}{\text{number of information bits per codeword}} \right). \quad (20)$$

where

$$P\{\mathbf{d}_i \rightarrow \mathbf{d}_j\} = P\left\{ \ln \left[ f(\mathbf{x}_i | \hat{\mathbf{c}}, \mathbf{d}_j) \right] \geq \max_{\mathbf{d}_k \in \Xi_d} \ln \left[ f(\mathbf{x}_i | \hat{\mathbf{c}}, \mathbf{d}_k) \right] \right\} \quad (21)$$

The event probability in (21) is computationally unattractive and analytically unsolvable because it contains too many decoding metric comparisons. An upper bound to (21) usually seen in the literature (e.g., [2, 4]) is given as

$$P\{\mathbf{d}_i \rightarrow \mathbf{d}_j\} \leq P_1\{\mathbf{d}_i \rightarrow \mathbf{d}_j\} = P\left\{ \ln \left[ f(\mathbf{x} | \hat{\mathbf{c}}, \mathbf{d}_j) \right] \geq \ln \left[ f(\mathbf{x} | \hat{\mathbf{c}}, \mathbf{d}_i) \right] \right\}. \quad (22)$$

Note that (21) is the exact event probability whereas (22) considers only the case  $\mathbf{d}_k = \mathbf{d}_i$  and is often a loose bound for the event probability. The prevalent traditional union bound (TUB) of BEP is calculated based on (22) as follows

$$BEP \leq \text{TUB} = \sum_{\mathbf{d}_j \in \Xi_d} P_1\{\mathbf{d}_i \rightarrow \mathbf{d}_j\} \left( \frac{\text{number of error bits in event } \mathbf{d}_i \rightarrow \mathbf{d}_j}{\text{number of information bits per codeword}} \right). \quad (23)$$

For fading cases where ideal interleaving is achieved (e.g., large Doppler spread and large interleaving depth), TUB is usually a tight bound of BEP. However, for the cases of interest in this work, i.e., a small Doppler spread and a finite interleaving depth, TUB is found to be a loose bound of the BEP. The TUB is loose for these conditions because the performance is dominated by the deep fades and when a deep fade occurs many symbol sequences are likely to have decoding metrics greater than that of the transmitted sequence and these sequences are not considered in (22). In Fig. 2, we evaluate the error performance of the BCM1 introduced in (1) with various fading rates., PSAM with  $P_{ins}=7$ , pilot symbol interpolation filter size  $(2N)=12$ , an interleaving depth  $D_{iv}=10$ , no transmitter diversity, and  $\gamma_b=14.65$  dB. The simulated BEP is obtained from 1,000,000

realizations of codewords for the considered channel conditions. The TUB is very loose in slow fading (small  $f_D T$ ) and is tight only when the normalized Doppler spread,  $f_D T$ , is relatively large. This significant bounding error is the motivation of our research on the improved union bounds in next section.

### C. Progressive Union Bound

The reduction of the bounding error of **TUB** is accomplished by simplifying (21) but not to the level of (22). The calculation of the pairwise error event probability is improved by increasing the number of decoding metric comparisons computed to bound (21). We propose considering  $K$  decoding metric comparisons instead of all decoding metric comparisons as in (21) or only one metric comparison as in (22). To this end, define the event

$$M_{k,j} = \left\{ \ln \left[ f(\mathbf{x} | \hat{\mathbf{c}}, \mathbf{d}_j) \right] \geq \ln \left[ f(\mathbf{x} | \hat{\mathbf{c}}, \mathbf{d}_k) \right] \right\} \quad (24)$$

and then

$$P_K \{ \mathbf{d}_i \rightarrow \mathbf{d}_j \} = P \left\{ \bigcap_{i=1}^K M_{k_i,j} \right\} \quad (25)$$

The approach using (25) which achieves the tightest bound of (21) is to pick the  $K$  events which include the decoding metric comparison of  $M_{i,j}$  ( $\mathbf{d}_j$  to  $\mathbf{d}_i$ ) and the metric comparison of  $M_{k,j}$  ( $\mathbf{d}_j$  to  $\mathbf{d}_k$ ) where  $\mathbf{d}_k$  is one of the  $K-1$  major competitive codewords of  $\mathbf{d}_j$  and  $\mathbf{d}_i$ . A competitive codeword of  $\mathbf{d}_j$  and  $\mathbf{d}_i$  implies a codeword whose distances from  $\mathbf{d}_j$  and  $\mathbf{d}_i$  are relatively small.

To evaluate (25) requires further analysis of the signal. From (19), it is straightforward to get

$$M_{k,j} = \left\{ \ln \left[ f(\mathbf{x} | \hat{\mathbf{c}}, \mathbf{d}_k) / f(\mathbf{x} | \hat{\mathbf{c}}, \mathbf{d}_j) \right] = -\delta_{kj} + \mathbf{z}^H \mathbf{Q}^{kj} \mathbf{z} \leq 0 \right\} \quad (26)$$

where

$$\begin{aligned} \delta_{kj} &= \ln\left[\det \mathbf{C}_k / \det \mathbf{C}_j\right], & \mathbf{z} &= \begin{bmatrix} \mathbf{x}_i^T & \hat{\mathbf{c}}^T \end{bmatrix}^T \\ \mathbf{Q}_{kj} &= \begin{bmatrix} \mathbf{C}_j^{-1} - \mathbf{C}_k^{-1} & \mathbf{C}_k^{-1} \boldsymbol{\Lambda}_{d_k} - \mathbf{C}_j^{-1} \boldsymbol{\Lambda}_{d_j} \\ \boldsymbol{\Lambda}_{d_k}^H \mathbf{C}_k^{-1} - \boldsymbol{\Lambda}_{d_j}^H \mathbf{C}_j^{-1} & \boldsymbol{\Lambda}_{d_j}^H \mathbf{C}_j^{-1} \boldsymbol{\Lambda}_{d_j} - \boldsymbol{\Lambda}_{d_k}^H \mathbf{C}_k^{-1} \boldsymbol{\Lambda}_{d_k} \end{bmatrix}. \end{aligned} \quad (27)$$

Hence (25) is equivalent to

$$P_K \left\{ \mathbf{d}_i \rightarrow \mathbf{d}_j \right\} = P \left\{ \mathbf{z}^H \mathbf{Q}_{kj} \mathbf{z} \leq \delta_{kj}, \quad k=1,2,\dots,K \right\}. \quad (28)$$

Note that the indexes ( $k_i$ 's) in (25) has been simplified in (28) to make the following derivation easier.

Define

$$\begin{aligned} g_{kj} &= \mathbf{z}^H \mathbf{Q}_{kj} \mathbf{z} & \mathbf{g} &= [g_{1j}, g_{2j}, \dots, g_{Kj}]^T & \boldsymbol{\delta} &= [\delta_{1j}, \delta_{2j}, \dots, \delta_{Kj}]^T \\ I_K(i, j) &= \left\{ g_{1j} \leq \delta_{1j}, \quad g_{2j} \leq \delta_{2j}, \quad \dots, g_{Kj} \leq \delta_{Kj} \right\} \end{aligned} \quad (29)$$

then

$$P_K \left\{ \mathbf{d}_i \rightarrow \mathbf{d}_j \right\} = \int_{I_K(i, j)} f(\mathbf{g}) d\mathbf{g}. \quad (30)$$

The density function in (30) can be expressed as

$$f(\mathbf{g}) = \frac{1}{(2\pi)^K} \int \phi(\mathbf{s}) \exp(\mathbf{s}^T \mathbf{g}) d\mathbf{s} \quad (31)$$

where (with the help of [24])

$$\mathbf{s} = [s_1, s_2, \dots, s_K]^T \quad (32)$$

$$\begin{aligned} \phi(\mathbf{s}) &= E \left[ \exp(-\mathbf{s}^T \mathbf{g}) \right] = E \left[ \exp \left( -\mathbf{z}^H (s_1 \mathbf{Q}_{1j} + \dots + s_K \mathbf{Q}_{Kj}) \mathbf{z} \right) \right] \\ &= 1 / \det \left[ \mathbf{I} + \mathbf{C}_z (s_1 \mathbf{Q}_{1j} + \dots + s_K \mathbf{Q}_{Kj}) \right]. \end{aligned} \quad (33)$$

and  $\mathbf{C}_z = \mathbf{E}[\mathbf{z}^H \mathbf{z}]$  is the covariance matrix of  $\mathbf{z}$ . Substituting (31) in (30) and switching order of integration (care must be taken in selecting contours to ensure the switch is valid) gives

$$P_K \{ \mathbf{d}_i \rightarrow \mathbf{d}_j \} = \frac{1}{(2\pi j)^K} \int \frac{\phi(s) \exp(\mathbf{s}^T \boldsymbol{\delta})}{s_1 s_2 \cdots s_K} ds. \quad (34)$$

If  $K=1$ , the integration in (34) is given as [25]

$$\frac{1}{2\pi j} \int_{s=\sigma-j\infty}^{\sigma+j\infty} \frac{\phi(s) e^{s\delta}}{s} ds = \begin{cases} -\sum \text{Residue}[\phi(s)e^{s\delta}/s]_{\text{Right Plane poles}}, & \text{if } \delta \leq 0 \\ \sum \text{Residue}[\phi(s)e^{s\delta}/s]_{\text{Left Plane poles} \cup \{0\}}, & \text{if } \delta > 0 \end{cases} \quad (35)$$

where  $\sigma$  is some constant satisfying  $0 < \sigma < \alpha$  the real part of the first right plane pole of  $\phi(s)$ . For  $K > 1$  cases, however, the analytical solution to (34) was not apparent and a numerical integration is required to get the results. This paper investigates  $K=2$  and 3 cases and defines the following progressive union bounds (PUB)

$$\text{2D-PUB} = \sum_{\mathbf{d}_i \in \Xi_d} \left\{ \left( \frac{\text{number of error bits in event } \mathbf{d}_i \rightarrow \mathbf{d}_j}{\text{number of information hits per codeword}} \right) \times \max_{\mathbf{d}_k \in \Xi_d} P \left\{ \mathbf{z}^H \mathbf{Q}_{ij} \mathbf{z} \leq \delta_{ij}, \mathbf{z}^H \mathbf{Q}_{kj} \mathbf{z} \leq \delta_{kj} \right\} \right\} \quad (36)$$

and

$$\text{3D-PUB} = \sum_{\mathbf{d}_j \in \Xi_d} \left\{ \left( \frac{\text{number of error bits in event } \mathbf{d}_i \rightarrow \mathbf{d}_j}{\text{number of information bits per codeword}} \right) \times \max_{\mathbf{d}_k, \mathbf{d}_i \in \Xi_d} P \left\{ \mathbf{z}^H \mathbf{Q}_{ij} \mathbf{z} \leq \delta_{ij}, \mathbf{z}^H \mathbf{Q}_{kj} \mathbf{z} \leq \delta_{kj}, \mathbf{z}^H \mathbf{Q}_{lj} \mathbf{z} \leq \delta_{lj} \right\} \right\}. \quad (37)$$

The maximization over  $\mathbf{d}_k$  and  $\mathbf{d}_i$  in (37) or the maximization over  $\mathbf{d}_k$  in (36) can be replaced by maximization over the major competitive codewords of  $\mathbf{d}_j$  and  $\mathbf{d}_i$  by looking at the distance profile on the signal constellation. The result of (35) can be applied to (36) and (37) and thus the two-dimensional numerical integration in (36) or three-dimensional numerical integration in (37) reduces to one-dimensional numerical integration in (36) and two-dimensional numerical integration in (37). Higher dimensional integration will achieve a tighter BEP bound but will require more computing complexity.

The performance of the progressive union bounds are shown in Figs. 2 and 3. The outcomes match the intuition that if more joint decoding metric comparisons are involved in the calculation of pairwise error event probability (i.e., using larger  $K$  in (25)), the BEP bound gets closer to the true BEP. Fig. 3 shows how these bounds perform in various SNR conditions where stationary fading ( $f_D=0$ ) and zero frequency offset ( $f_o=0$ ) are considered. If  $\text{BEP}=0.01$  is interested, a 6 dB SNR/bit bounding loss of TUB is found in Fig. 3. 2D-PUB and 3D-PUB outperform the TUB 2 dB and 3 dB in SNR/bit respectively and this fact proves the significance of the progressive union bound. In the remainder of the paper where we will evaluate the BEP with PSAM under various conditions of transmitter diversity, the 2D-PUB is employed.

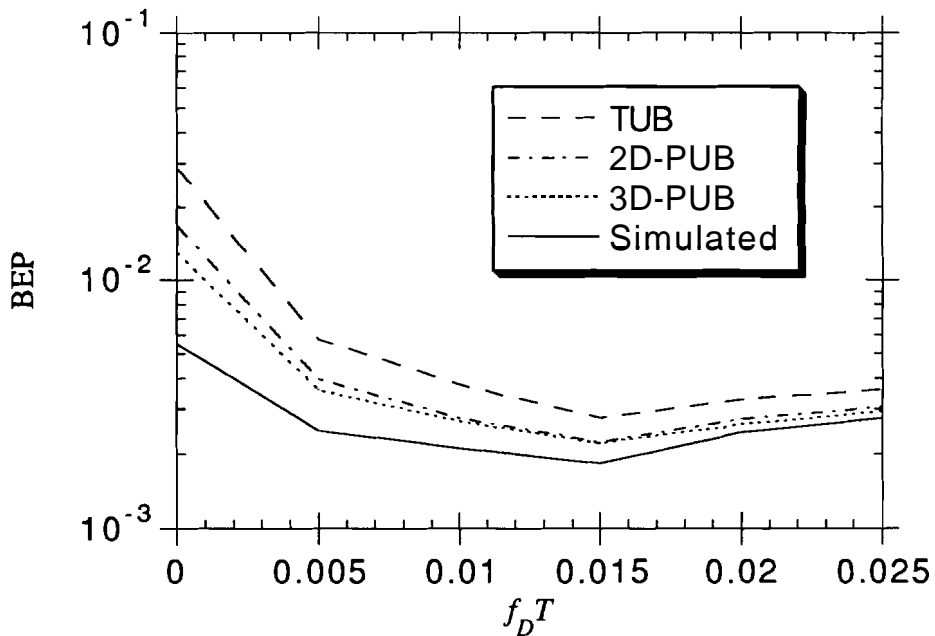


Fig. 2. Bounding errors in various fading rates. A case of  $\gamma_b=14.65$  dB, no diversity, and interleaving depth = 10 is considered.

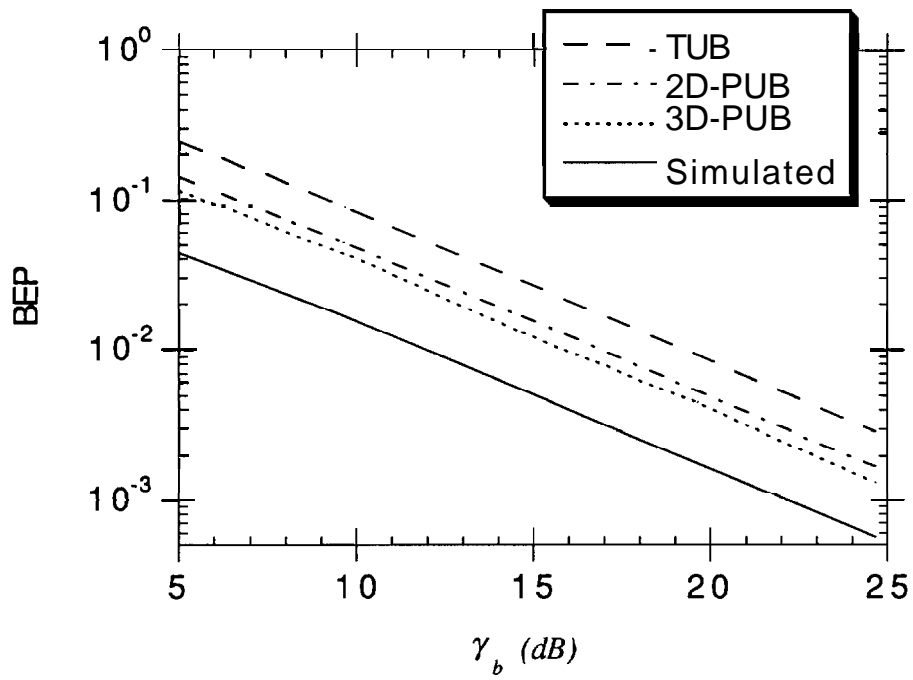


Fig. 3. Bounding errors in stationary fading ( $f_D=0$ ). A case of no diversity ( $f_o=0$ ) and interleaving depth = 10 is considered.

## IV. Performance of Transmitter Diversity

As introduced in section II, the purpose of using intentional frequency offset in transmitter diversity is to introduce the enforced time-varying fading in the received signal.. From the point of view for performance analysis, the effect of using intentional frequency offset in transmitter diversity is actually only addition of the terms  $\cos(2\pi f_o \tau)$  and/or  $\cos(2\pi f_o \tau/3)$  to the autocorrelation function of the MD process in (8)-(10). The effect of these terms will be analyzed in detail in the following.

### A. Achieving Ideal Interleaving

Ideal interleaving (independent fading on each code symbol) provides the best performance with coded modulations. This condition implies that the autocorrelation of the MD samples at any two code symbols be equal to zero, i.e.,

$$\text{Ideal Interleaving} \Leftrightarrow E[c_k c_l^*] = E_b \delta_{k-l} \quad (38)$$

where  $k$  and  $l$  are any two time indexes of a transmitted codeword. As we can see in (4) that if transmitter diversity is not used, then in a very slow fading situation (i.e.,  $f_D$  is close to zero), the autocorrelation of the MD process remains at a value close to  $E_b$  for large values of  $\tau$  and ideal interleaving cannot be achieved in this case unless a very large buffer in the receiver can be used and a long processing delay is tolerable.

The transmitter diversity technique using intentional frequency offset provides a practical solution for providing independent fading. Fig. 4 illustrates the autocorrelation function (normalized to  $E_b$ ) of the MD process for various transmitter diversities (multiple antennas) in a stationary fading ( $f_D=0$ ) situation. Two features can be observed from Fig. 4. First, the autocorrelation function of the MD process drops quickly as the

displacement goes large, and second, the more antennas we use, the farther the autocorrelation goes before it returns to the highly correlated areas ( $\pm 1$ ). The most important characteristic is that using more antennas can generate more zero crossing points in the autocorrelation of MD before it goes back to the highly correlated areas ( $\pm 1$ ). Since we place the tones (offset frequencies for different antennas:) with uniform separation in the frequency spectrum over a fixed bandwidth (see Section II-C), these zero crossing points are also uniformly separated (periodic) to the extent of  $L$  (space diversity). This property is very significant since 1) the most prevalent interleaver uses an array processor which produces the uniformly interleaved codeword and 2) to satisfy (38) requires the correlation of MD be zero at the displacement of any multiples (up to a certain extent) of the interleaving depth ( $D_{iv}$ ).

As a result, (38) is now achievable in any fading situation even a stationary fading situation if the frequency offset and the interleaving depth are properly selected. From Fig. 4 and (8)-(10), we can see that, for space diversity =  $L$

$$f_o D_{iv} T = \frac{L-1}{2L} \Rightarrow \text{Ideal Interleaving for time diversity} = L \quad (39)$$

Here we should distinguish two diversity terminologies, space diversity and time diversity. We define the space diversity is the number of antennas used in the transmitter diversity with the frequency offset described in Section II-C. The time diversity is defined as the number of the independently faded code symbols inside a codeword. (39) provides the criterion for achieving ideal interleaving with the flexibility of tradeoff between bandwidth expansion and buffer size with processing delay. If only a small bandwidth expansion ( $f_o$ ) is allowed,  $D_{iv}$  must be large enough to accommodate the ideal interleaving. On the other hand, if the processing delay is highly restrictive or the buffer size in the receiver is a constraint, then a larger bandwidth expansion needs to be used to obtain ideal interleaving.

Also from (39) and Fig. 4, we can see that

$$\text{achievable time diversity} \leq \text{space diversity used.} \quad (40)$$

This implies 1) if a time diversity =  $L$  is needed, at least  $L$  antennas must be used, and 2) if only time diversity  $\leq L$  is needed (typically for BCM cases with block length =  $L$ ), using  $L$  antennas with (39) can achieve the needed time diversity and using more than  $L$  antennas will not improve the performance.

#### A-1 Comparison between BCM and TCM for ideal interleaving

It becomes obvious now that one advantage of using BCM compared to TCM is that BCM only requires a finite time diversity (equal to its block length) to achieve ideal interleaving whereas TCM has infinitely long coded sequences and hence ideal interleaving with TCM is theoretically not feasible in slow fading.

However, in the performance analysis of TCM [2], the effect of error events with longer length are usually neglected since their contribution to the BEP are trivial and therefore pseudo ideal interleaving for TCM can be attained by fulfilling a time diversity to the extent of the length of significant error events. Take the TCM in [11] (denoted as TCM1) as an example. The Hamming distance of TCM1 is equal to 3 and the performance analysis only considered the error events up to length 5. Hence a time diversity of 5 or 6 should be good enough to achieve the pseudo ideal interleaving. A similar pseudo ideal interleaving idea can be applied to the longer block length BCM.

#### **B. Non-ideal Interleaving Performance**

Since achieving ideal interleaving for a BCM with block length  $L$  requires  $L$  antennas and for a TCM calls for much more antennas, analysis for non-ideal interleaving deserves attention. Especially for real world applications where higher order and longer length coded modulations are proposed and/or used (e.g., Reed-Solomon BCM, 128-state 128-

QAM TCM etc.), ideal interleaving in slow fading is more difficult to **attain**.

### **B-1. Example of BCM1**

To illustrate the gain of using transmitter diversity with intentional frequency offset, a simple case of BCM is studied in this section. Another advantage (besides the finite time diversity requirement) of using BCM is the simplicity of BEP performance analysis since the number of trellis paths of BCM are finite. Fig. 5 shows the effect on BEP (2D-PUB) of BCM1 by using frequency offset with varying interleaving depth in stationary fading ( $f_D=0$ ) and  $\gamma_b = 14.65$  dB. PSAM with  $P_{ins}=7$ , a Wiener filter of length 12 and  $f_o T=0.005$  are considered. The optimal points of  $f_o D_{iv} T$  (which yield the lowest BEP) for space diversity=3 and 4 are  $1/3$  and  $3/8$  respectively. The results match the zero crossing points in Fig. 4 and (39). Fig. 5 also demonstrates space diversity of 4 achieves the same lowest BEP as space diversity of 3 and this fact also matches our above argument about ideal interleaving that the block length of BCM1 equals 3 so that more than 3 antennas will not improve the performance if ideal interleaving has already been achieved. The optimal points of  $f_o D_{iv} T$  for space diversity=2 is around 0.12. Note that ideal interleaving is not achieved for space diversity=2 in BCM1 since the time diversity required by BCM1 is 3.

Fig. 6 shows the performance gain of using intentional frequency offset with transmitter diversity in stationary fading. Again PSAM with  $P_{ins}=7$  and a Wiener filter of length 12 are considered. Optimal  $f_o D_{iv} T$  (from Fig. 5) are used for each space diversity case. Shown in Fig. 6 are the simulated BEP (from 1,000,000 realization of codewords for the channel conditions) in the lower curve of each group and the 2D-PUB in the upper curve of each group. If a design BEP is  $10^{-3}$ , then around 8-10 dB SNR/bit gain is obtained by using two transmitting antennas with optimal  $f_o D_{iv} T$  compared to the case of one transmitting antenna (no diversity). A further 2 dB SNR/bit gain can be **acquired** if one more transmitting antenna with optimal  $f_o D_{iv} T$  is used. Also from Fig. 6, the bounding error of 2D-PUB is significantly reduced in the cases that transmitter diversity with proper  $f_o D_{iv} T$  is used.

## B-2. Example of TCM1

In this section, the TCM1 (in [11]) is considered. TCM1 outputs 16-QAM with 16-state where the in-phase part and the quadrature-phase part are independently but identically generated by a 4-state 4-PAM trellis code. TCM1 has Hamming distance 3 and code rate =  $1/2$ . Fig. 7 shows the effect on BEP (2D-PUB) of TCM1 by using frequency offset with varying interleaving depth in stationary fading ( $f_D=0$ ) and  $\gamma_b=14.65$  dB. PSAM with  $P_{ins}=7$ , a Wiener filter of length 12 and  $f_oT=0.005$  are again considered. The optimal points of  $f_oD_{iv}T$  (which yield the lowest BEP) for space diversity=2, 3, 4 are 0.1, 0.23, and 0.36 respectively. Since error events of length 5 still contributes significantly to the BEP, pseudo ideal interleaving is not achieved by using space diversity=2, 3, or 4 but the lowest achievable BEP is progressively reduced because the possibility of finding 4 periodic points in the domain of  $f_o\mathcal{S}$  (in Fig. 4) that all have close to zero value of autocorrelation of MD in Fig. 4 is higher if larger space diversity is used. Based on the optimal  $f_oD_{iv}T$  found in Fig. 7, Fig. 8 illustrates the performance gain of using intentional frequency offset with transmitter diversity for TCM1 in stationary fading. Again PSAM with  $P_{ins}=7$  and a Wiener filter of length 12 are considered. If a design BEP is  $10^{-3}$ , then around 10 dB SNR/bit gain is obtained by using two transmitting antennas with proper  $f_oD_{iv}T$  compared to the case of one transmitting antenna (no diversity). A further 3 or 5 dB SNR/bit gain can be acquired if 3 or 4 transmitting antennas with optimal  $f_oD_{iv}T$  is used.

## B-3 Degradation caused by Ideal Interleaving Assumption

In this section, we investigate the performance degradation caused by the assumption of ideal interleaving in the case that ideal interleaving is actually not achieved. The purpose for this is that if the assumption of ideal interleaving is valid, the decoding complexity is greatly reduced because the  $\mathbf{C}_c$  matrix in (17) and thus the  $\mathbf{C}_i, \mathbf{C}_j, \mathbf{C}_k$  in

(27) are then diagonal matrixes. A simpler form of decoding metric (compared to (26)) is obtained as

$$\begin{aligned} \text{metric}_k &= -\ln[f(\mathbf{x}|\hat{\mathbf{c}}, \mathbf{d}_k)] + \lambda \\ &= \ln \left[ \prod_{l=1}^M \left( |d_{kl}|^2 E[c_l - \hat{c}_l]^2 + N_0 \right) \right] + \sum_{l=1}^M \frac{|x_l - d_{kl}\hat{c}_l|^2}{|d_{kl}|^2 E[c_l - \hat{c}_l]^2 + N_0} \end{aligned} \quad (41)$$

where  $\lambda$  is some constant and M is the length of the codeword. For coded modulation that has independent but identical in-phase and quadrature phase part of output symbols, the decoding metric in (41) can be further simplified and divided into the in-phase and quadrature phase parts. That is, if high quality estimates of MD samples are obtained (e.g., a longer Wiener filter or a smaller pilot insertion period is used etc.), (41) can be approximated as

$$\text{metric}_k = \sum_{l=1}^M |x_l - d_{kl}\hat{c}_l|^2 = \sum_{l=1}^M |\hat{c}_l|^2 \left( \text{Re} \left[ \frac{x_l}{\hat{c}_l} \right] - \text{Re}[d_{kl}] \right)^2 + \sum_{l=1}^M |\hat{c}_l|^2 \left( \text{Im} \left[ \frac{x_l}{\hat{c}_l} \right] - \text{Im}[d_{kl}] \right)^2. \quad (42)$$

Separated decisions on in-phase and quadrature phase parts can then be made and the complexity can be greatly reduced if modulations on the in-phase and quadrature phase parts are generated independently (e.g., TCM1).

Fig. 9 and 10 show the error performance (2D-PUB) of using optimal decoding (26) or decoding by (41) for BCM1 and TCM1 respectively. Again PSAM with  $P_{ins}=7$  and a Wiener filter of length 12 are considered. Space diversity=2 and optimal  $f_oD_{iv}T$  is evaluated for BCM1 case in Fig. 9. The SNR/bit degradation of using simpler decoding (41) as if ideal interleaving is achieved is around 1 dB for BCM1. Space diversity=2 and 3 with respective optimal  $f_oD_{iv}T$  are considered for TCM1 case in Fig. 10. The SNR/bit degradation of using simpler decoding (41) as if ideal interleaving is achieved is around 1 dB (for space diversity=2) or 0.4 dB (for space diversity=3) respectively.

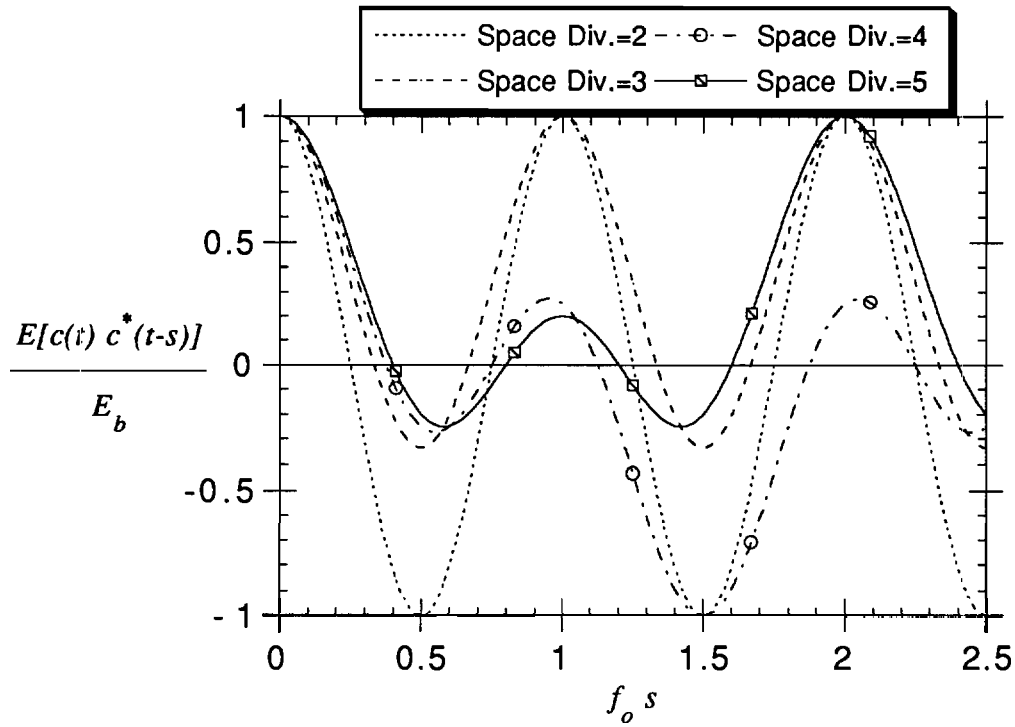


Fig. 4. Autocorrelation of the MD process in stationary fading.

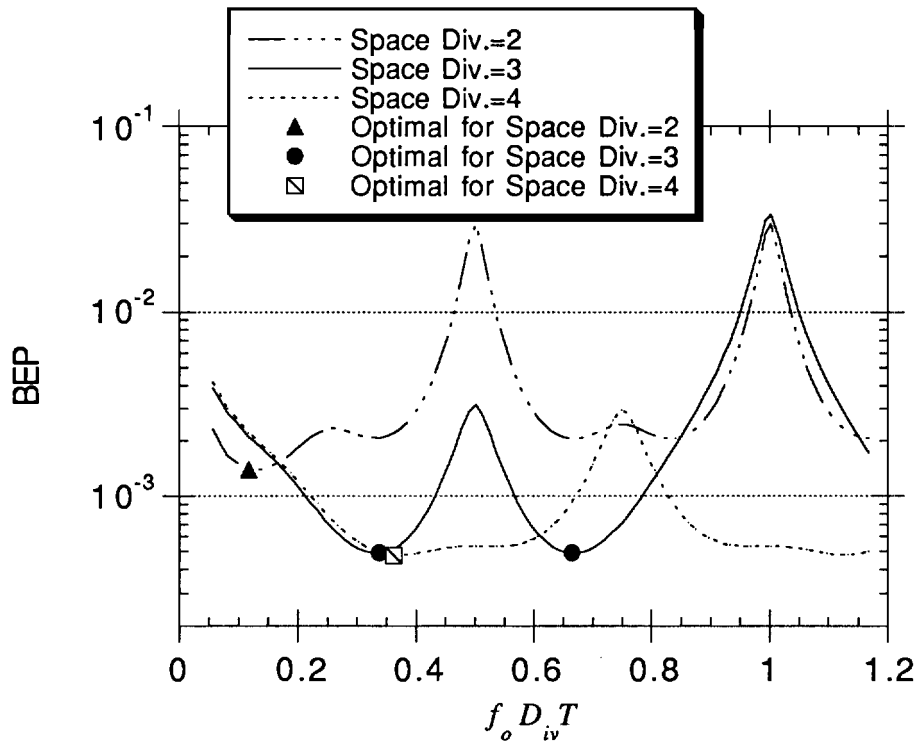


Fig. 5. The effect of frequency offset and interleaving depth in stationary fading. Shown is the 2D-PUB of BCM1 at  $\gamma_b=14.65$  dB.

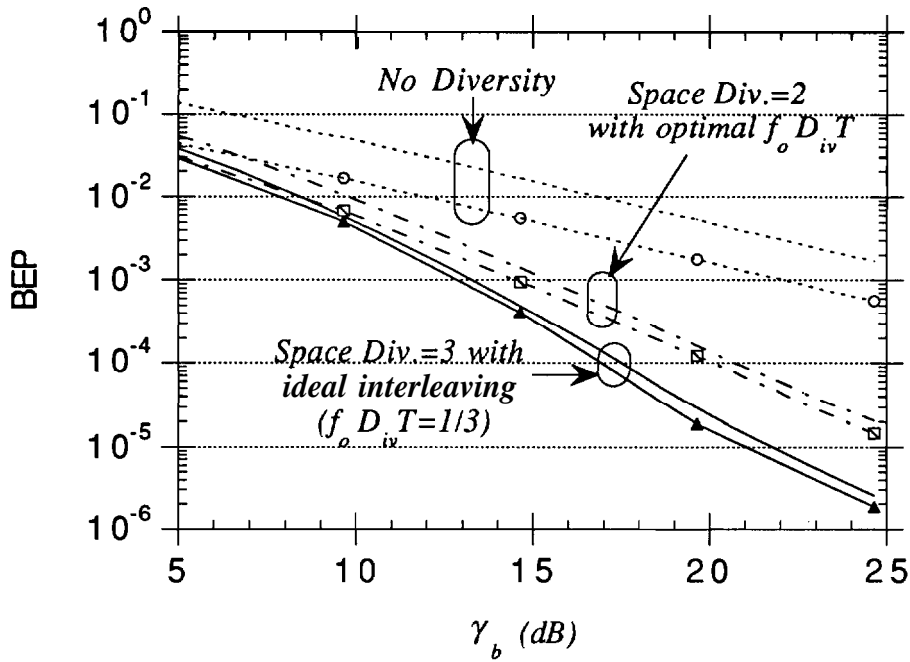


Fig. 6. Performance gain of transmitter diversity for BCM1 in stationary fading. Shown are the: 2D-PUB (upper curve of each group) and the simulated BEP (lower curve of each group).

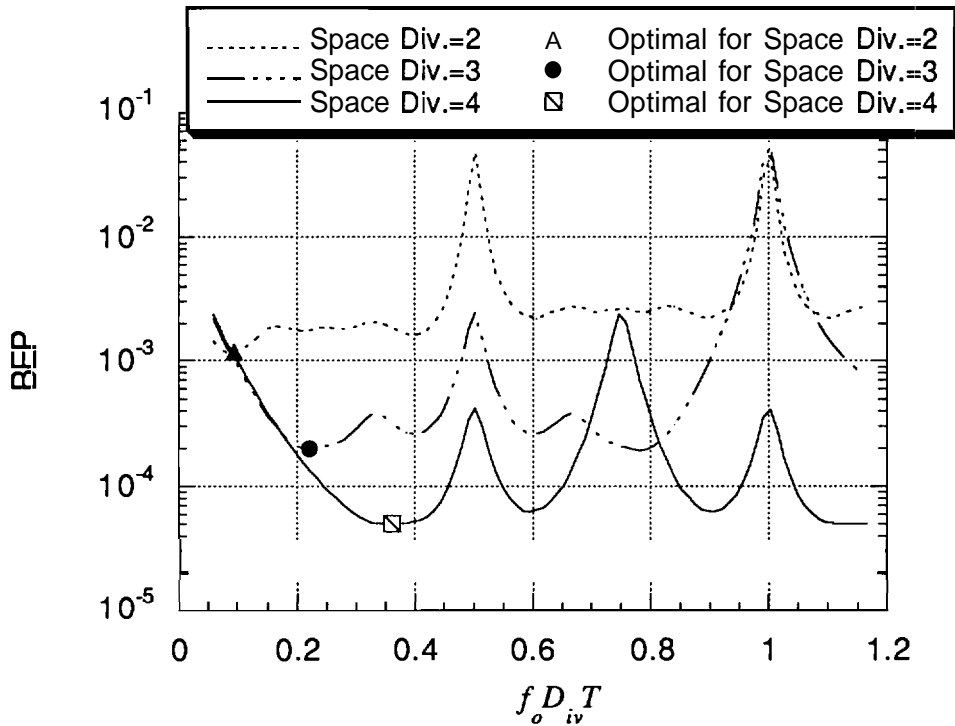


Fig. 7. The effect of frequency offset and interleaving depth in stationary fading for TCM1. Shown is the 2D-PUB at  $\gamma_b=14.65$  dB.

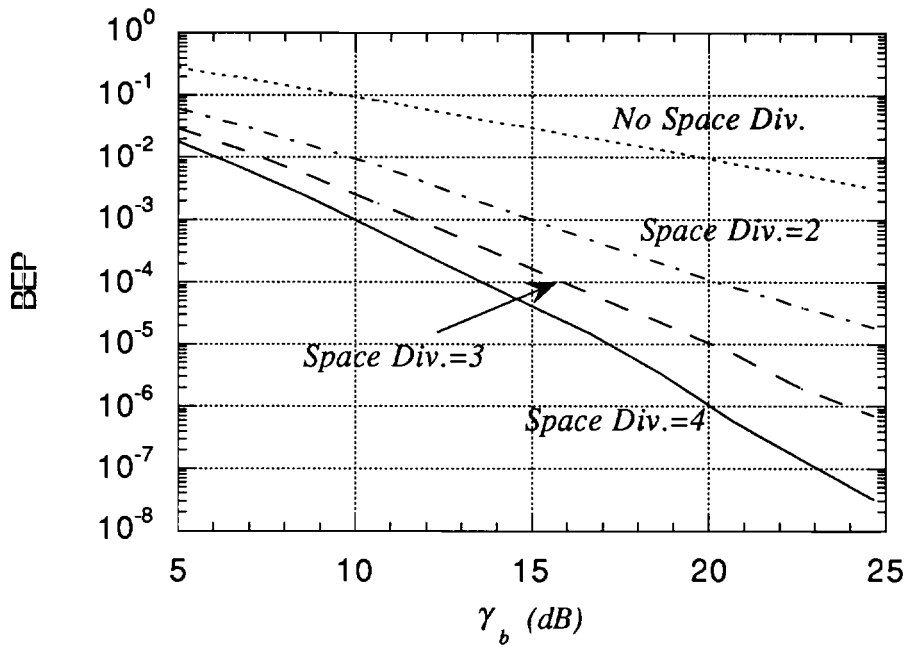


Fig. 8. Performance gain of using transmitter diversity for the TCM1 in stationary fading. The optimal  $f_o D_{iv} T$  (from Fig. 7) is used for each space diversity case.

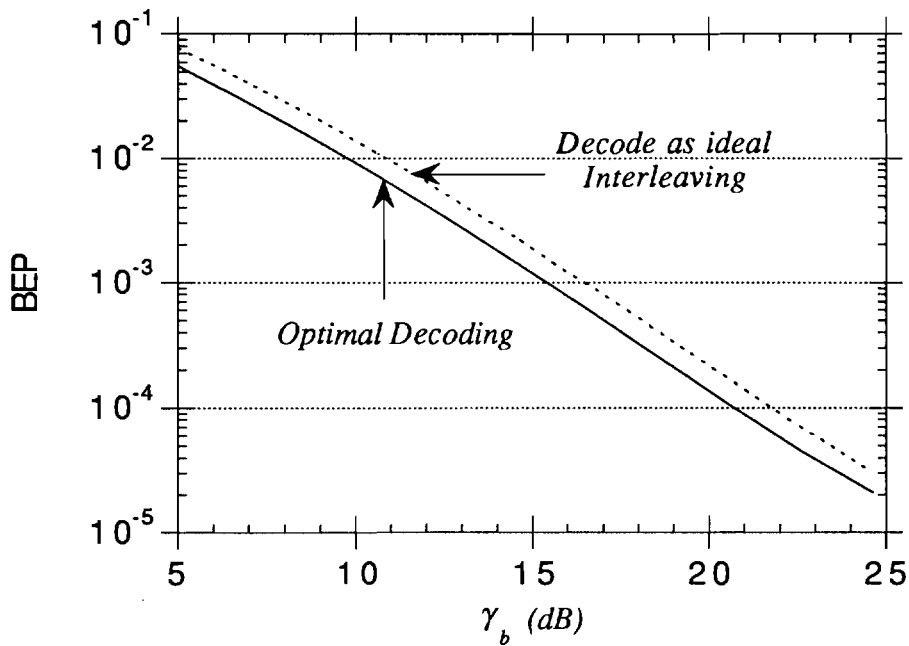


Fig. 9. Performance degradation caused by the assumption of ideal interleaving for BCM1. Space Div. = 2 is considered and the 2D-PUB is shown.

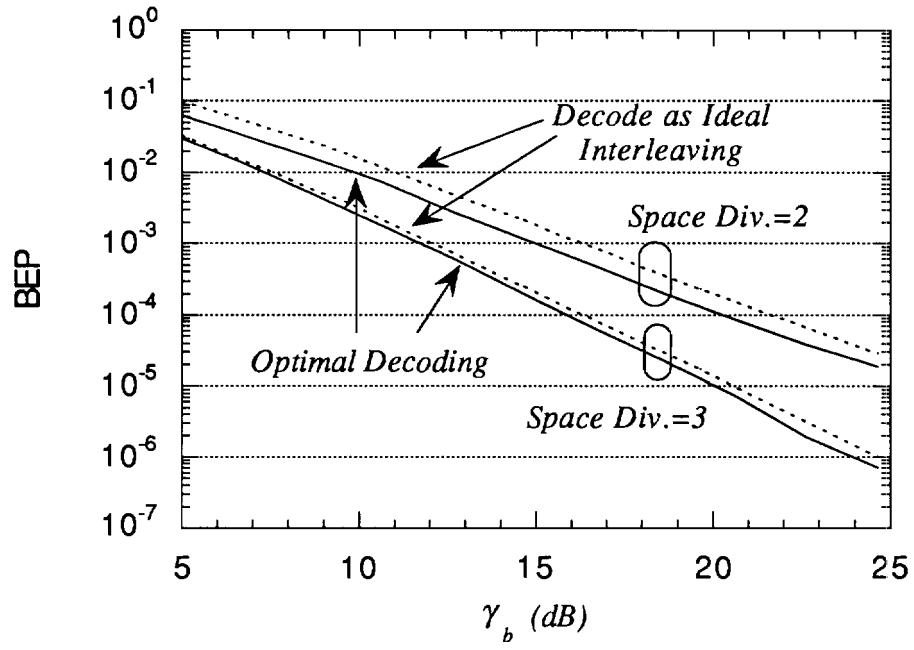


Fig. 10. Performance degradation caused by the assumption of ideal interleaving for the TCM1.

## VI Conclusion

Performance analysis of coded modulation in correlated fading **typically** for a slow fading environment instead of an independent fading is established in this paper. The traditional union bound prevalent in the error performance analysis of communication **systems** is found only to yield a loose bound of BEP for coded modulation in correlated fading or a slow fading situation. Progressive union bounds which include more joint decoding metric comparisons in the error event probability calculation are proposed in this **paper** to provide an improved BEP bound for performance analysis in a slow fading environment.

The transmitter diversity technique using intentional frequency **offset** to produce time-varying fading is fully investigated in this paper. Ideal interleaving for coded modulation previously assumed in the literature is actually not feasible in slow fading especially in stationary fading if the transmitter diversity technique is not used. By proper selection of the intentional frequency offset and the interleaving depth, ideal interleaving in any fading situations is now achievable. Design criteria of the transmitter diversity technique using intentional frequency offset are also introduced. For a less **diversity** case (space diversity < time diversity required), the optimal frequency offset and interleaving depth can be searched by the performance analysis tools developed in this paper. When the optimal frequency offset and interleaving depth are used, the **performance** gain of the transmitter diversity using intentional frequency offset is found to be significant and is illustrated in this paper with certain examples.

## List of References

- [1] D. Divsalar and M.K. Simon, "Trellis Coded Modulation for 4800-9600 bits/s Transmission Over a Fading Mobile Satellite Channel," *IEEE J. Select Areas Commun.*, vol. SAC-5, February 1987, pp. 162-175.
- [2] J.K. Cavers and P. Ho, "Analysis of the Error Performance of Trellis-Coded Modulation in Rayleigh Fading Channels," *IEEE Trans. Commun.*, vol. COM-40, January 1992, pp. 74-83.
- [3] E. Biglieri, et al., *Introduction to Trellis-Coded Modulations with Applications*, Macmillan, New York, 1991.
- [4] C. Tellambura, Q. Wang, and V.K. Bhargava, "A Performance Analysis of Trellis-Coded Modulation Schemes Over Rician fading Channels," *IEEE Trans. Veh. Tech.*, vol. VT-42, November 1993, pp. 491-501.
- [5] S.H. Jamali and T. Le-Ngoc, "Performance Comparison of Different Decoding Strategies for a Bandwidth-Efficient Block-Coded Scheme on Mobile Radio Channels," *IEEE Trans. Veh. Technol.*, vol. VT-41, November 1992, pp. 505-515.
- [6] H.S. Jamali and T. Le-Ngoc, "Bandwidth Efficient Communication Via a Rayleigh Fading Channel Using RS Coded Multiphase Signaling," *IEEE Trans. Commun.*, vol. COM-41, November 1993, pp. 1594-1597.
- [7] S.S. Soliman and K. Mokrani., "Performance of Coded System:; Over Fading Dispersive Channels," *IEEE Trans. Commun.*, vol. COM-40, January 1992, pp. 51-59.
- [8] N. Seshadri and J.H. Winters, "Two Signaling Schemes for Improving the Error Performance of Frequency-Division-Duplex Transmission System Using Transmitter Antenna Diversity," *Intl. J. Wireless Info. Network*, Vol. 1, 1994, pp. 49-60.
- [9] A. Wittneben, "A New Bandwidth Efficient Transmit Antenna Modulation Diversity Scheme for Linear Digital Modulation," *IEEE International Conference on Communications, Geneva, Switzzland*, 1993, pp. 1630-1634.
- [10] A. Hiroike, F. Adachi, and N. nakajima, "Combined Effects of Phase Sweeping Transmitter Diversity and Channel Coding," *IEEE Trans. Veh. Tech.*, VT-41, May 1992, pp. 170-176.
- [11] P. Ho, J. Cavers, and J. Varaldi, "The Effect of Constellation Density on Trellis Coded Modulation in Fading Channels," *IEEE Trans. Veh. Technol.*, vol. VT-42, August 1993, pp. 318-325.

- A. Aghamohammadi and H. Meyr, "A New Method for Phase Synchronization and Automatic Gain Control for Linearly Modulated Signals on Frequency Flat Fading Channels," *IEEE Trans. Commun.*, vol. COM-38, January 1991, pp. 25-29.
- [13] J.K. Cavers, "An Analysis of Pilot Symbol Assisted Modulation for Rayleigh Faded Channels," *IEEE Trans. Veh. Technol.*, vol. VT-40, November 1991, pp. 686-693.
- [14] M.L. Moher and J.H. Lodge, "TCMP - A Modulation and Coding Scheme for Rician Fading Channels," *IEEE J. Select. Areas Commun.*, vol. SAC-7, December 1989, pp. 1347-1355.
- [15] J.K. Cavers, "Performance of Tone Calibration with Frequency Offset and Imperfect Pilot Filter," *IEEE Trans. Veh. Technol.*, vol. VT-40, May 1991, pp. 426-434.
- [16] M.P. Fitz, "A Dual-Tone Reference Digital Demodulator for Mobile Digital Communications," *IEEE Trans. Veh. Technol.*, vol. VT-42, May 1993, pp. 156-165.
- [17] F. Davarian, "Mobile Digital Communication Via Tone Calibration," *IEEE Trans. Veh. Tech.*, vol. VT-36, May 1987, pp. 55-62.
- [18] P. Ho and D. Fung, "Error Performance of Multiple-Symbol Differential Detection of PSK Signals Transmitted Over Correlated Rayleigh Fading Channels," *IEEE Trans. Commun.*, vol. COM-40, October 1992, pp. 1566-1569.
- [19] D. Divsalar and M.K. Simon, "Multiple-Symbol Differential Detection of MPSK," *IEEE Trans. Commun.*, vol. COM-38, March 1990, pp. 300-308.
- [20] W.C. Jakes, *Microwave Mobile Communications*, Wiley, New York, 1974.
- [21] J.K. Cavers, "On the Validity of the Slow and Moderate Fading Models for Matched Filter Detection of Rayleigh Fading Signals," *Canadian Journal of Electrical and Computer Engineering*, vol. 17, October 1992, pp. 183-189.
- [22] T. Hattori and S. Ogose, "A new Modulation Scheme for Multitransmitter Simulcast Digital Mobile Radio Communication," *IEEE Trans. Veh. Tech.*, VT-29, May 1980, pp. 260-270.
- [23] F. Adachi, "Transmitter Diversity for a Digital FM Paging System," *IEEE Trans. Veh. Tech.*, VT-28, 1979, pp. 333-338.
- [24] G.L. Turin, "The characteristic function of Hermitian quadratic forms in complex normal variables," *Biometrika*, 1960, pp. 199-201.
- [25] N.W. McLachlan, *Complex Variable Theory and Transform Calculus*, Cambridge University Press, 1953.